Journal of Medicinal Chemistry

Article

pubs.acs.org/jmc

Head-to-Head Prenyl Tranferases: Anti-Infective Drug Targets

Fu-Yang Lin,[†] Yi-Liang Liu,[†] Kai Li,[‡] Rong Cao,[†] Wei Zhu,[†] Jordan Axelson,[‡] Ran Pang,[§] and Eric Oldfield*[,†,‡]

[†]Center for Biophysics and Computational Biology, [‡]Department of Chemistry, and [§]School of Molecular and Cellular Biology, University of Illinois at Urbana-Champaign, Urbana, Illinois 61801, United States

Supporting Information

ABSTRACT: We report X-ray crystallographic structures of three inhibitors bound to dehydrosqualene synthase from *Staphylococcus aureus*: **1** (BPH-651), **2** (WC-9), and **3** (SQ-109). Compound **2** binds to the S2 site with its −SCN group surrounded by four hydrogen bond donors. With **1**, we report two structures: in both, the quinuclidine headgroup binds in the allylic (S1) site with the side chain in S2, but in the presence of PPi and Mg^{2+}, the quinuclidine's cationic center interacts with PPi and three Mg^{2+}, mimicking a transition state involved in diphosphate ionization. With **3**, there are again two structures. In one, the geranyl side chain binds to either S1 or S2 and the adamantane headgroup binds to S1. In the second, the side chain binds to S2 while the headgroup binds to S1. These results provide structural clues for the mechanism and inhibition of the head-to-head prenyl transferases and should aid future drug design.

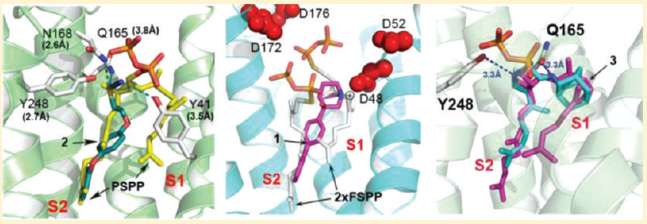

INTRODUCTION

There is currently considerable interest in the structure, function, and inhibition of the "head-to-head" class of prenyl tranferase enzymes that condense farnesyl diphosphate to squalene or dehydrosqualene.[1] These reactions are carried out by squalene synthase (SQS) in humans and in some protozoa such as *Trypanosoma cruzi* or by dehydrosqualene synthase (CrtM) in *Staphylococcus aureus* (SaCrtM) (Figure 1). Inhibiting SQS in protozoa is of interest, since it blocks formation of the essential membrane sterol ergosterol, while blocking human SQS (HsSQS) lowers cholesterol levels; plus, it results in formation of antibacterial neutrophil extracellular traps (NETs).[2] Also of interest is the observation that inhibiting SaCrtM inhibits biofilm formation[3] with *S. aureus*, in addition to preventing formation of the virulence factor staphyloxanthin (Figure 1), leading to immune system based bacterial killing.[4] There is thus interest in the development of compounds that might inhibit more than one target (e.g., combining NETs/biofilm/STX activity or direct protozoal killing + NETs formation), and here, we present crystal structures of three SQS/CrtM inhibitors bound to CrtM, together with mechanistic insights into the SQS/CrtM mode of action. The inhibitors investigated are of interest, since two are known to inhibit SQS while the third has an unknown mechanism of action but has been used in clinical trials, and here, we show that it can serve as a lead for inhibiting both CrtM and SQS.

RESULTS AND DISCUSSION

In the case of the quinuclidine **1**[5−7] (Figure 2), a known potent squalene synthase inhibitor, we obtained two new structures of **1** bound to SaCrtM. Electron density results are shown in Supporting Information Figure S1A,B. In the first, Figure 3A (PDB code 4E9Z), **1** binds with its cationic headgroup in the S1 (cationic/donor) site while the biphenyl side chain binds very close to S2. The cationic center is ∼1.9 Å from C2 in the S1 farnesyl side chain (Figure 3A). In the second structure, Figure 3B (PDB code 4EA0), the side chain occupies a site between the S1 and S2 FSPP binding sites while the cationic center is now 2.5 Å from C1, 1.7 Å from C2, and 0.7 Å from C3 in the (overlaid, white) S1 FSPP (Figure 3B). Both structures strongly suggest that the quinuclidine is acting as an isostere for the S1 farnesyl carbocation. In the second structure (PDB code 4EA0) there is also a PPi group as well as three Mg^{2+}, with the (inorganic) PPi being close to the position occupied by the diphosphate group in the S1 FSPP structure;[4] plus, two of the three Mg^{2+} (Mg_A^{2+}, Mg_B^{2+}) seen in the FSPP structure are observed (Figure 3B). These results are consistent with the proposal that the initial FPP ionization step occurs in the S1 site,[8] and are reminiscent of the observation that cationic bisphosphonate inhibitors of other prenyl synthases, such as FPP synthase (FPPS), have their cationic, anionic, and Mg^{2+} located in very similar positions, as shown in the **4**/FPPS[9] superimposition in Figure 3C. Notably, this S1/cationic site structure is quite distinct from that reported previously for **1** (via soaking, as opposed to cocrystallization), in which the quinuclidine carbocation feature was located in essentially the same position as the cyclopropane ring in PSPP (Figure 3D), where it mimics a second transition state. So the quinuclidine

Received: February 15, 2012
Published: April 9, 2012

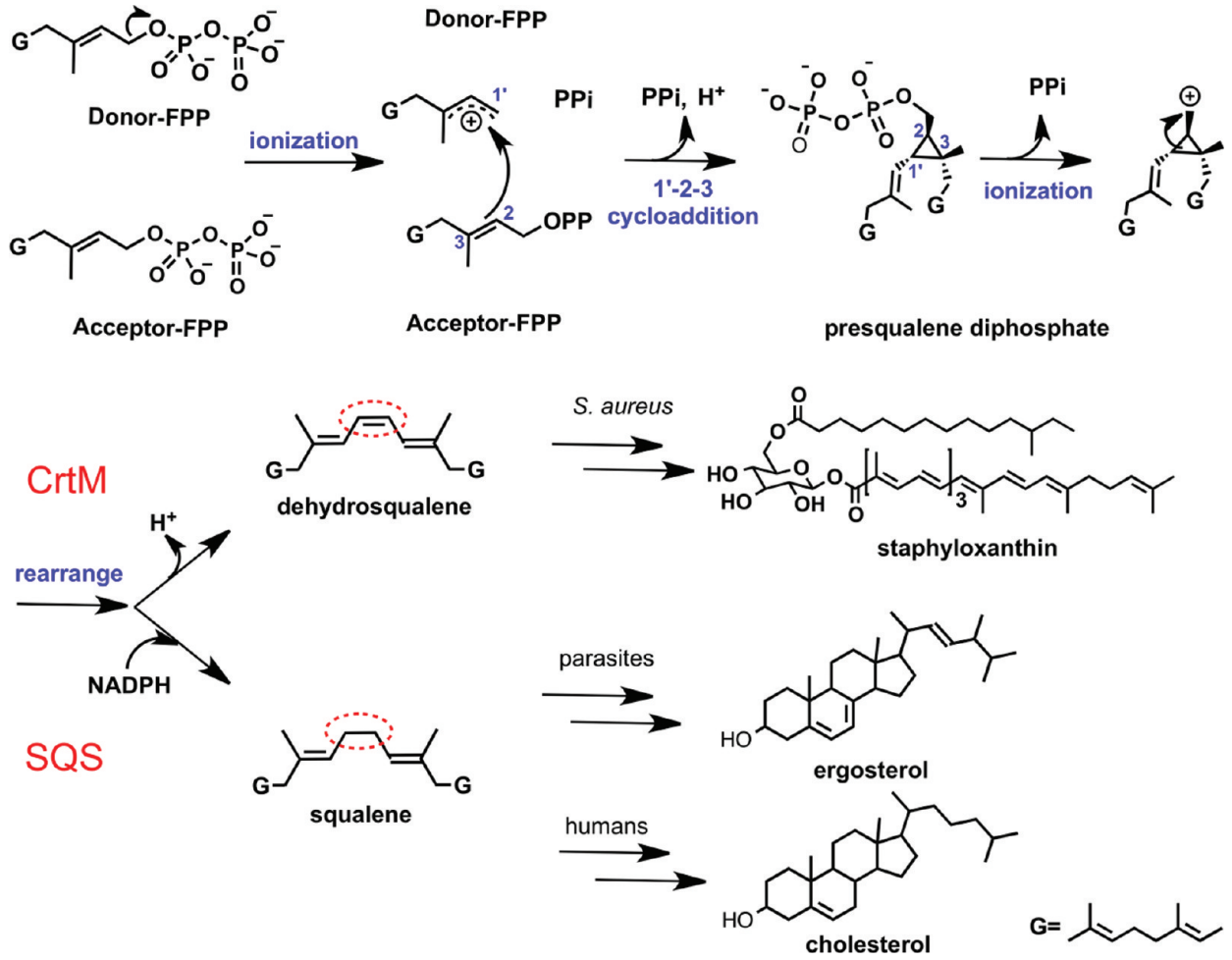

Figure 1. Schematic of the first and second half reactions catalyzed by CrtM and SQS leading to formation of dehydrosqualene and squalene and later conversion of these products to staphyloxanthin, ergosterol, and cholesterol.

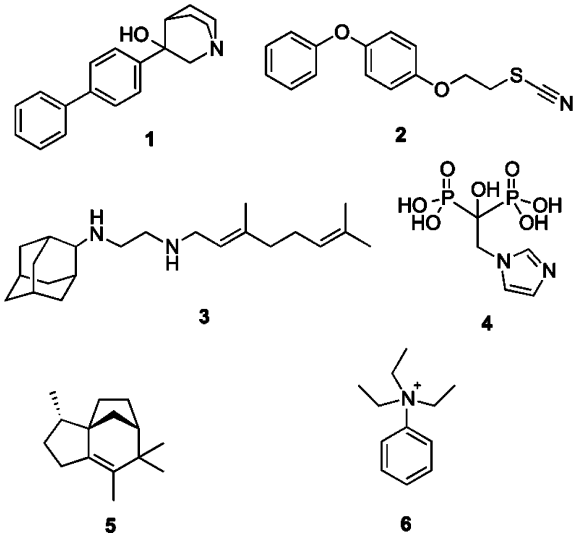

Figure 2. Chemical structures of small molecule inhibitors.

(**1**) can block either the S1 or S2 headgroup site, opening up new possibilities for inhibitor design.

The **1**-PPi-$[Mg^{2+}]_3$ structure (Figure 3B) is also of considerable interest, since it bears a strong resemblance (in terms of placement of the cationic center, PPi and $[Mg^{2+}]_3$ groups) to the recently reported structure[10] of the terpene cyclase, epi-isozizaene (**5**) synthase, containing a bound inhibitor, **6** (benzyltriethylammonium, Figure 2). As can be seen in the superposition shown in Figure 3E, both structures lack the $[Mg_C^{2+}]$ seen in the CrtM/FSPP structure[4] and contain instead a new Mg^{2+}, Mg_D^{2+} (parts E and F of Figure 3). The rmsd of the N^+, PPi, and three Mg^{2+} in the CrtM and epi-isozizaene structures is only 0.35 Å, supporting the idea that diphosphate ionization of FPP in the head-to-head prenyl transferases, as well as in the terpene cyclase, is dominated by the same driving force, a $[Mg^{2+}]_3$-PPi interaction. The results obtained with the **1**-PPi-$[Mg^{2+}]_3$ structure are also of interest, since they help clarify the role of Y129 in CrtM (Y171 in HsSQS), which is among the most essential residues needed for catalytic activity (based on mutagenesis[8,11] and a SCORECONS analysis[12]). In earlier work, it was thought that this residue (in HsSQS) might be involved in stabilizing the farnesyl cation via a cation–π interaction; however, this residue is ~8.5 Å from the proposed cationic center. In the **1**-PPi-$[Mg^{2+}]$ structure, we now see that the Tyr-OH is hydrogen-bonded to a water molecule that coordinates to one of the Mg^{2+} seen in the X-ray structure, Mg_D^{2+} (Figure 3F (in blue)). This suggests that Y129 may help stabilize and/or facilitate removal of the diphosphate group rather than directly stabilizing the S1 carbocation.

dx.doi.org/10.1021/jm300208p | J. Med. Chem. 2012, 55, 4367–4372

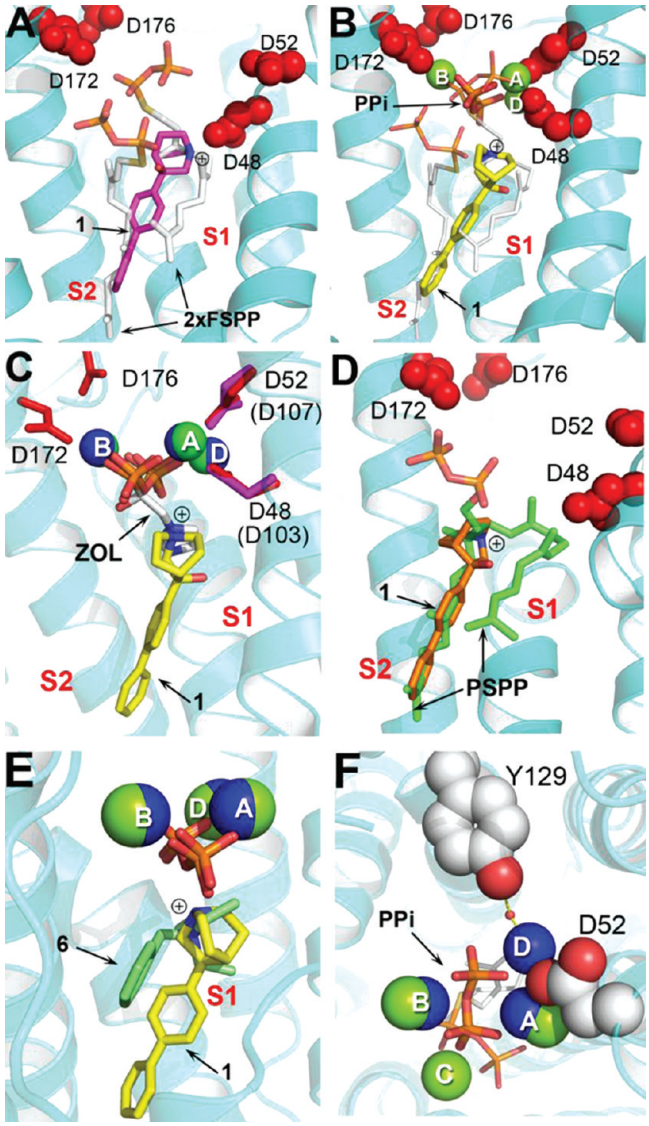

Figure 3. X-ray crystallographic structures of **1** bound to CrtM. (A) CrtM/**1** (no Mg^{2+}, PPi; PDB code 4E9Z). Cationic (N^+) center (blue) is close to S1 FPP C3. FSPP is superimposed in white. (B) CrtM/**1** + Mg^{2+} + PPi (PDB code 4EA0). Cationic center is close to the putative S1 allylic carbocation. N^+ is also close to the PPi group. (C) As in (B) but superimposed on zoledronate/Mg^{2+} ligand from FPPS structure (PDB code 2F8C). (D) **1** occupying S2 carbocation center (PDB code 3ACW), superimposed on PSPP structure (PDB code 3NPR). (E) Structure from (B) superimposed on **6**/Mg^{2+}/PPi from epi-isozizaene synthase (PDB 3KB9). (F) Top view of (B) showing Y129-H_2O-$Mg_D{}^{2+}$ and PPi-Mg^{2+} interactions. The ligand is *S*-thiolofarnesyl diphosphate.

We show in Figure 4 the single crystal X-ray crystallographic structure of the thiocyanate **2**[13] bound to CrtM. **2** is a potent SQS inhibitor of interest in treating Chagas disease.[14,15] Electron density results are shown in Figure S1C, and full crystallographic data acquisition and structure refinement results are in Table 1. The molecule inhibits CrtM with K_i = 1.5 μM (Figure S2A) and binds with its diphenyl ether side chain occupying the S2 site normally occupied by the acceptor FPP or one of the PSPP side chains, as seen in the **2** (cyan)-PSPP (yellow) superposition in Figure 4B. This side chain binding site can also be occupied by several other inhibitors, including the phosphonosulfonates,[4] and is completely hydrophobic. The

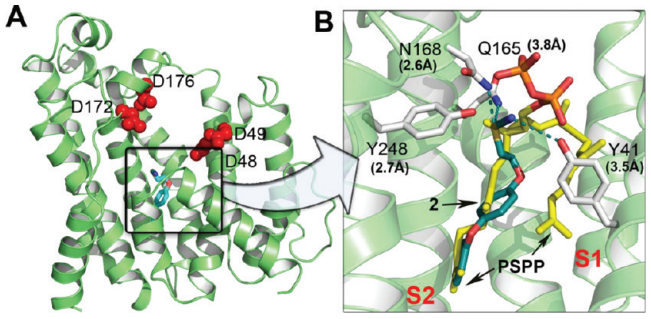

Figure 4. X-ray crystallographic structure of **2** bound to CrtM (PDB code 4E9U). (A) **2** binds to a buried, hydrophobic S2 site. (B) **2** (in cyan) is superimposed on the PSPP reaction intermediate (yellow) bound to CrtM.

question then arises as to the nature of the interactions undergone by the thiocyanate group. Unlike the quinuclidine inhibitors, the thiocyanate group cannot be charged; however, alkyl thiocyanates can act as proton acceptors because of the following resonance scheme:

$$R{-}S{-}C{\equiv}N \leftrightarrow R{-}S^{+}{=}C{=}N^{-}$$

There is a $\Delta H = -6.5$ kJ mol^{-1} interaction between phenol and CH_3SCN.[16] In the **2**/CrtM crystal structure (PDB code 4E9U), there are four polar residues close to the thiocyanate nitrogen (Y41, Q165, N168, and Y248) with, on average, an SCN–protein distance of ~3.2 Å (Figure 4B). Since all of these amino acid side chains are polar, it seems likely that they will contribute to ligand binding via electrostatic (hydrogen bonding) interactions, in much the same way that, for example, phenol interacts with the thiocyanate group in liquid MeSCN.[16]

The question then arises as to whether **2** binds to *Trypanosoma cruzi* SQS (TcSQS) in the same manner as it does to CrtM. To date, there are no structures of TcSQS. However, there are 11 residues in CrtM (F22, Y41, A134, V137, G138, L141, A157, G161, L164, Q165, and N168) that are close (<4 Å) to **2** in the CrtM structure, and these residues are totally conserved in both HsSQS and TcSQS. This strongly suggests that the ligand will bind into the same S2 pocket in TcSQS, with the same polar interactions with the thiocyanate group as in CrtM.

Finally, we determined two structures of **3** bound to CrtM. **3** is a novel, dialkylated ethylendiamine with an adamantyl "headgroup" and a geranyl "side chain" that potently inhibits the growth of *Candida albicans*, *Aspergillus fumigatus*, *Mycobacterium tuberculosis*, and *Helicobacter pylori* and has progressed through phase Ia clinical trials.[17] The actual enzyme targets involved have not been reported. Nevertheless, on the basis of the general similarities (large hydrophobic group–cation center–small hydrophobic group) between the quinuclidine (**1**) and **3** structures, it seemed possible that **3** might inhibit CrtM and SQS. This is the case, with K_i values of 0.36 μM (CrtM), 0.74 μM (hSQS), and 1.2 μM (TcSQS) (Figure S2). We show in Figure 5A two crystallographic structures of **3** bound to CrtM, one obtained by cocrystallization (PDB code 4EA1), the other by soaking (PDB code 4EA2). Electron density results are shown in Figure S1D,E. In the cocrystal structure, we found two alternative conformations, with the geranyl side chain binding to either the S1 or S2 site, the ethylenediamine linker interacting with either D48 or Q165, and the adamantane headgroup being solvent exposed (Figures S3 and S4). In the structure obtained by soaking, **3** adopts a "bent" conformation with the adamantane headgroup binding

dx.doi.org/10.1021/jm300208p | J. Med. Chem. 2012, 55, 4367–4372

Table 1. Data Collection and Refinement Statistics for CrtM with 1, 2, and 3

	crystal (PDB code)				
	2/CrtM (soaking) (4E9U)	**1**/CrtM (cocrystal) (4E9Z)	**1**/CrtM-PPi-Mg^{2+} (cocrystal) (4EA0)	**3**/CrtM (cocrystal) (4EA1)	**3**/CrtM (soaking) (4EA2)
			Data Collection		
radiation source	APS 21-ID-F	APS 21-ID-F	APS 21-ID-F	APS 21-ID-F	APS 21-ID-F
wavelength (Å)	0.97857	0.97857	0.97857	0.97857	0.97857
space group	$P3_221$	$P3_221$	$P3_121$	$P3_221$	$P3_221$
a (Å)	80.4	80.6	80.3	80.6	80.1
b (Å)	80.4	80.6	80.3	80.6	80.1
c (Å)	90.8	91.8	180.8	91.6	90.9
resolution (Å)[a]	50.0−2.10 (2.14−2.10)	50.0−2.06 (2.12−2.06)	50.0−2.12 (2.17−2.12)	50.0−2.46 (2.50−2.46)	50.0−2.02 (2.09−2.05)
no. of reflections[a]	20218 (966)	21572 (1041)	37084 (1169)	12795 (583)	21470 (858)
completeness (%)[a]	99.9 (98.9)	99.9 (100)	94.5 (61.1)	99.2 (91.0)	98.5 (80.9)
redundancy[a]	10.1 (4.90)	12.7 (12.7)	8.8 (6.1)	9.5 (5.4)	10.1 (5.0)
R_{merge} (%)[a]	10.1 (65.2)	7.30 (45.0)	7.60 (59.7)	8.80 (44.1)	6.5 (68.9)
$I/\sigma(I)$ [a]	21.3 (1.56)	44.0 (5.04)	27.7 (1.52)	2.69 (1.74)	41.8 (1.5)
			Refinement		
resolution (Å)[a]	36.8−2.1 (2.21−2.10)	30.0−2.08 (2.12−2.06)	50.0−2.12 (2.17−2.12)	30.0−2.46 (2.17−2.12)	34.7−2.05 (2.10−2.05)
no. of reflections[a]	19540 (2320)	20373 (1228)	35058 (1687)	12091 (819)	20270 (1246)
R_{work} (%)[a]	18.9 (21.8)	19.1 (20.8)	22.2 (31.5)	23.2 (34.8)	20.6 (27.2)
R_{free} (%)[a]	23.6 (26.5)	24.1 (24.7)	27.8 (36.3)	31.4 (34.8)	26.0 (31.7)
			Geometry Deviation		
bond length (Å)	0.007	0.015	0.005	0.006	0.014
bond angle (deg)	0.962	1.331	0.692	0.912	1.234
			Mean *B*-Value (Å^2)/Number of Non-Hydrogen Atoms		
all refined atoms	38.5/2568	34.0/2602	46.2/5046	42.3/2456	48.76/2467
compound atoms	49.7/19	58.1/21	38.4/42	34.9/48	71.8/24
Mg ions			28.5/6		75.6/1
water molecules	38.5/156	40.8/184	41.6/186	40.6/47	52.4/63
			Ramachandran Plot (%)		
most favored	98.6	98.2	96.6	96.4	96.8
additionally allowed	1.06	1.07	2.84	1.8	2.2
generously allowed	0.35	0.71	0.53	1.8	1.0

[a]Values in the parentheses are for the highest resolution shells.

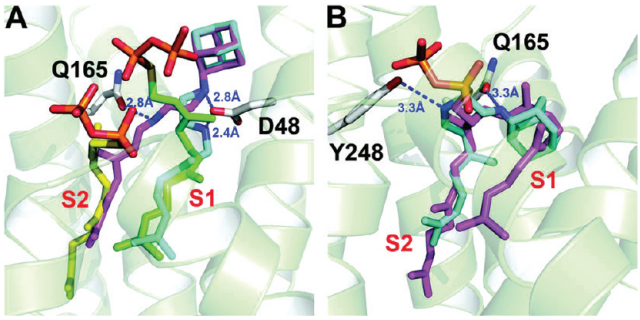

Figure 5. X-ray crystallographic structure of **3** bound to CrtM. (A) Structure obtained by cocrystallization (PDB code 4EA1) showing that geranyl side chain can occupy both S1 and S2 sites (cyan, S1; magenta, S2), superimposed on the FSPP structures (green, yellow; PDB code 2ZCP). (B) Structure obtained by soaking (PDB code 4EA2). The inhibitor **3** (cyan) adopts a bent conformation with the adamantane headgroup occupying the same site as the "bend" in the PSPP (magenta) intermediate, in S1 (PDB code 3NPR).

to the S1 site, close to the position occupied by the quinuclidine headgroup in **1**, and the geranyl side chain is located in the S2 site (Figure 5B and Figure S5. In this structure, the hydrophobic headgroup occupies the same pocket as occupied by the "bend" in presqualene diphosphate (or FSPP), as can be seen in the superimposition shown in Figure 5B (PSPP in magenta). Since **3** has been successfully tested in humans, the observation that it inhibits both human and *T. cruzi* SQS as well as *S. aureus* CrtM clearly makes it an interesting potential lead for further development as an SQS/CrtM inhibitor.

■ CONCLUSIONS

The results presented here are of interest for several reasons. First, we have obtained the structure of the potent antiparasitic thiocyanate drug lead **2**, which inhibits squalene synthase, bound here to a dehydrosqualene synthase (Figure 4). The biphenyl ether side chain binds to the S1 site, and the thiocyanate group is involved in an extensive series of electrostatic interactions with protein residues. There are 11 residues in close contact with the ligand, and these residues are all conserved in *S. aureus* CrtM, human SQS, and *T. cruzi* SQS, supporting binding of this inhibitor to the S2 pocket the SQS enzymes as well. Second, we report two structures of the quinuclidine (**1**), bound to dehydrosqualene synthase. One structure (**1** + PPi/Mg) is of particular interest, since it mimics a transition state in which the cationic center formed on FPP (or PSPP) ionization is in S1, while the exiting PPi binds to a new $[Mg^{2+}]_3$ cluster, with one Mg^{2+} close to the highly conserved Y129, which we propose is positioned to facilitate PPi

dx.doi.org/10.1021/jm300208p | *J. Med. Chem.* 2012, 55, 4367−4372

removal. Third, we find that the anti-infective drug **3** inhibits both CrtM and SQS (Figure S2). We obtained two CrtM structures. In one, the geranyl side chain binds to either the S1 or S2 site, the ethylenediamine interacts with essential protein residues, and the adamantane group is solvent exposed (Figure 5A). In the second (Figure 5B), the geranyl side chain occupies the S2 site while the adamantane group is now buried and occupies the same position as the "bend" in the S1 PSPP side chain.[8]

Overall, these results are of significance, since they provide new structural information on the mechanism of action and inhibition of the head-to-head prenyl transferases that are of interest as novel anti-infective drug targets. Such inhibitors may target not only direct pathogen killing[6,13,18] but also innate immune system-based killing, via virulence factor inhibition,[4] NET formation,[2] and biofilm inhibition.[3]

EXPERIMENTAL SECTION

Materials. All chemicals were purchased from Sigma-Aldrich (St. Louis, MO) or Alchem Laboratories Corp. and were used as provided. BL-21 (DE3) competent cells were purchased from Stratagene (La Jolla, CA). Syntheses of **1**−**3** (Figure 2) were as reported previously.[15,19,20] The CrtM plasmid was provided by Andrew H.-J. Wang's group. The human SQS (HsSQS) and *Trypanosoma cruzi* SQS (TcSQS) plasmids were provided by Dolores Gonzalez-Pacanowska.

Protein Expression, Purification, and Crystallization. Protein expression, purification, and crystallization were as described previously.[4,6,8]

Inhibition Assays. CrtM, TcSQS, and hSQS inhibition assays were as described previously.[4,8]

Crystallographic Aspect. Structures were obtained as described in detail previously.[4,8] Structure figures were made by using PyMOL,[21] and ligand−protein interaction figures were made using MOE.[22]

ASSOCIATED CONTENT

Supporting Information

Electron density maps for inhibitors bound to CrtM (Figure S1), dose−response curves for CrtM inhibition (Figure S2), and protein−ligand interactions for CrtM/**3** (Figures S3−S5). This material is available free of charge via the Internet at http://pubs.acs.org.

Accession Codes

The atomic coordinates and structure factors have been deposited in the RCSB Protein Data Bank for CrtM complexed with **2** (PDB code 4E9U), **1** (PDB code 4E9Z), **1**/PPi-Mg^{2+} (PDB code 4EA0), and **3** (PDB codes 4EA1 and 4EA2).

AUTHOR INFORMATION

Corresponding Author

*Phone: (217) 333-3374. Fax: (217) 244-0997. E-mail: eo@chad.scs.uiuc.edu.

Notes

The authors declare no competing financial interest.

ACKNOWLEDGMENTS

This work was supported by NIH Grant AI-074233 to E.O. We thank A. H.-J. Wang and C.-I. Liu for providing their CrtM plasmid, and D. Gonzalez-Pacanowska for hSQS and TcSQS plasmids. We thank Y. Gao for his assistance with protein crystallization. Use of the Advanced Photon Source was supported by the U.S. Department of Energy, Office of Science, Office of Basic Energy Sciences, under Contract DE-AC02-06CH111357. Use of the Life Science Collaborative Access Team Sector 21 was supported by the Michigan Economic Development Corporation and the Michigan Technology Tri-Corridor (Grant 085P1000817).

ABBREVIATIONS USED

CrtM, dehydrosqualene synthase; SQS, squalene synthase; FPP, farnesyl diphosphate; FPPS, farnesyl diphosphate synthase; FSPP, *S*-thiolofarnesyl diphosphate; PSPP, presqualene diphosphate; PPi, diphosphate; NET, neutrophil extracellular trap

REFERENCES

(1) Oldfield, E.; Lin, F.-Y. Terpene biosynthesis: modularity rules. *Angew. Chem., Int. Ed.* **2011**, *50*, 2−16.

(2) Chow, O. A.; von Kockritz-Blickwede, M.; Bright, A. T.; Hensler, M. E.; Zinkernagel, A. S.; Cogen, A. L.; Gallo, R. L.; Monestier, M.; Wang, Y.; Glass, C. K.; Nizet, V. Statins enhance formation of phagocyte extracellular traps. *Cell Host Microbe* **2010**, *8*, 445−454.

(3) Lopez, D.; Kolter, R. Functional microdomains in bacterial membranes. *Genes Dev.* **2010**, *24*, 1893−1902.

(4) Liu, C. I.; Liu, G. Y.; Song, Y.; Yin, F.; Hensler, M. E.; Jeng, W. Y.; Nizet, V.; Wang, A. H.; Oldfield, E. A cholesterol biosynthesis inhibitor blocks *Staphylococcus aureus* virulence. *Science* **2008**, *319*, 1391−1394.

(5) Fernandes Rodrigues, J. C.; Concepcion, J. L.; Rodrigues, C.; Caldera, A.; Urbina, J. A.; de Souza, W. In vitro activities of ER-119884 and E5700, two potent squalene synthase inhibitors, against *Leishmania amazonensis*: antiproliferative, biochemical, and ultrastructural effects. *Antimicrob. Agents Chemother.* **2008**, *52*, 4098−4114.

(6) Sealey-Cardona, M.; Cammerer, S.; Jones, S.; Ruiz-Perez, L. M.; Brun, R.; Gilbert, I. H.; Urbina, J. A.; Gonzalez-Pacanowska, D. Kinetic characterization of squalene synthase from *Trypanosoma cruzi*: selective inhibition by quinuclidine derivatives. *Antimicrob. Agents Chemother.* **2007**, *51*, 2123−2129.

(7) Urbina, J. A.; Concepcion, J. L.; Caldera, A.; Payares, G.; Sanoja, C.; Otomo, T.; Hiyoshi, H. In vitro and in vivo activities of E5700 and ER-119884, two novel orally active squalene synthase inhibitors, against *Trypanosoma cruzi*. *Antimicrob. Agents Chemother.* **2004**, *48*, 2379−2387.

(8) Lin, F. Y.; Liu, C. I.; Liu, Y. L.; Zhang, Y.; Wang, K.; Jeng, W. Y.; Ko, T. P.; Cao, R.; Wang, A. H.; Oldfield, E. Mechanism of action and inhibition of dehydrosqualene synthase. *Proc. Natl. Acad. Sci. U.S.A.* **2010**, *107*, 21337−42.

(9) Rondeau, J. M.; Bitsch, F.; Bourgier, E.; Geiser, M.; Hemmig, R.; Kroemer, M.; Lehmann, S.; Ramage, P.; Rieffel, S.; Strauss, A.; Green, J. R.; Jahnke, W. Structural basis for the exceptional in vivo efficacy of bisphosphonate drugs. *ChemMedChem* **2006**, *1*, 267−273.

(10) Aaron, J. A.; Lin, X.; Cane, D. E.; Christianson, D. W. Structure of epi-isozizaene synthase from *Streptomyces coelicolor* A3(2), a platform for new terpenoid cyclization templates. *Biochemistry (Moscow)* **2010**, *49*, 1787−1797.

(11) Gu, P.; Ishii, Y.; Spencer, T. A.; Shechter, I. Function−structure studies and identification of three enzyme domains involved in the catalytic activity in rat hepatic squalene synthase. *J. Biol. Chem.* **1998**, *273*, 12515−12525.

(12) Valdar, W. S. Scoring residue conservation. *Proteins* **2002**, *48*, 227−241.

(13) Urbina, J. A.; Concepcion, J. L.; Montalvetti, A.; Rodriguez, J. B.; Docampo, R. Mechanism of action of 4-phenoxyphenoxyethyl thiocyanate (WC-9) against *Trypanosoma cruzi*, the causative agent of Chagas' disease. *Antimicrob. Agents Chemother.* **2003**, *47*, 2047−2050.

(14) Cinque, G. M.; Szajnman, S. H.; Zhong, L.; Docampo, R.; Schvartzapel, A. J.; Rodriguez, J. B.; Gros, E. G. Structure−activity relationship of new growth inhibitors of *Trypanosoma cruzi*. *J. Med. Chem.* **1998**, *41*, 1540−1554.

(15) Elhalem, E.; Bailey, B. N.; Docampo, R.; Ujvary, I.; Szajnman, S. H.; Rodriguez, J. B. Design, synthesis, and biological evaluation of aryloxyethyl thiocyanate derivatives against *Trypanosoma cruzi*. *J. Med. Chem.* **2002**, *45*, 3984−3999.

(16) Igarashi, K.; Watari, F.; Aida, K. Hydrogen bonding between phenol and alkyl thiocyanates. *Spectrochim. Acta. A* **1969**, *25*, 1743.
(17) Rivers, E. C.; Mancera, R. L. New anti-tuberculosis drugs in clinical trials with novel mechanisms of action. *Drug Discovery Today* **2008**, *13*, 1090−1098.
(18) Cammerer, S. B.; Jimenez, C.; Jones, S.; Gros, L.; Lorente, S. O.; Rodrigues, C.; Rodrigues, J. C.; Caldera, A.; Ruiz Perez, L. M.; da Souza, W.; Kaiser, M.; Brun, R.; Urbina, J. A.; Gonzalez Pacanowska, D.; Gilbert, I. H. Quinuclidine derivatives as potential antiparasitics. *Antimicrob. Agents Chemother.* **2007**, *51*, 4049−4061.
(19) Orenes Lorente, S.; Gomez, R.; Jimenez, C.; Cammerer, S.; Yardley, V.; de Luca-Fradley, K.; Croft, S. L.; Ruiz Perez, L. M.; Urbina, J.; Gonzalez Pacanowska, D.; Gilbert, I. H. Biphenylquinuclidines as inhibitors of squalene synthase and growth of parasitic protozoa. *Bioorg. Med. Chem.* **2005**, *13*, 3519−3529.
(20) Onajole, O. K.; Govender, P.; van Helden, P. D.; Kruger, H. G.; Maguire, G. E.; Wiid, I.; Govender, T. Synthesis and evaluation of SQ109 analogues as potential anti-tuberculosis candidates. *Eur. J. Med. Chem.* **2010**, *45*, 2075−2079.
(21) *The PyMOL Molecular Graphic System*, version 1.3; Schrödinger, LLC: Portland, OR.
(22) *Molecular Operating Environment (MOE)*, version 2009.10; Chemical Computing Group, Inc: Montreal, Canada.